CURRENT BIOCHEMISTRY
ISSN: 2355-7877
e-ISSN: 2355-7931
Journal homepage: http://journal.ipb.ac.id/index.php/cbj
Journal E-mail: current.biochemistry@gmail.com

Analysis In Silico of Red Ginger (*Zingiber officinale* var. Rubrum) Active Compounds as Acetylcholinesterase Inhibitor

Mega Safithri[1,2*], Djarot Sasongko[3] and Astrit Afrilia[4]

[1]*Bioanalysis Division, Department of Biochemistry, IPB University, Bogor, 16680, Indonesia*
[2]*Tropical Biopharmaca Research Center (Biopharmaca), Institute for Research and Community Service, IPB University, Bogor, Indonesia*
[3]*Biomolecule Division, Department of Biochemistry, IPB University, Bogor, 16680, Indonesia*
[4]*Department of Biochemistry, IPB University, Bogor, 16680, Indonesia*

Received: *June 23, 2026;* Accepted: *December 31, 2024*

Corresponding author e-mail: safithri@apps.ipb.ac.id

ABSTRACT

Treatment using acetylcholinesterase (AChE) inhibitors has been widely used, but these drugs still have many side effects. In vitro research related to red ginger has shown potential as an AChE inhibitor, but the compounds and their in silico interactions are unknown. This study aims to identify the active compounds in red ginger that have the potential to inhibit AChE and to analyze the interactions that occur in silico. The active compound of red ginger from the literature was tethered to the AChE receptor, then the bioavailability and toxicity of the ligands were predicted and their interactions were analyzed. The results showed that galanthamine (natural ligand), donepezil, and rivastigmine (comparison ligand) had ΔG values of -10.5710, -10.3260 and -7.3670 kcal/mol and Ki of 0.0175, 0.0265, and 3.9261 μM, the best inhibition potential is owned by fisetin and morin ligands with ΔG of -10.4250 and -10.3570 kcal/mol and Ki of 0.0224 and 0.0251 μM. Both ligands have more negative ΔG values than the comparison ligands and bind strongly to the active site on the HIS447 amino acid residue, so they can potentially act as competitive inhibitors of the AChE enzyme and are easily soluble and not toxic to the body.

Keywords: *acetylcholinesterase inhibitors; dementia; red ginger*

ABSTRAK

Pengobatan menggunakan inhibitor asetilkolinesterase (AChE) telah banyak dilakukan, namun obat tersebut masih memberikan banyak efek samping. Penelitian secara in vitro terkait jahe merah telah terbukti berpotensi sebagai inhibitor AChE, namun belum diketahui senyawa dan interaksinya secara in silico. Penelitian ini bertujuan mengidentifikasi senyawa aktif jahe merah yang berpotensi menginhibisi AChE serta analisis interaksi yang terjadi secara in silico. Senyawa aktif jahe merah dari literatur ditambatkan ke reseptor AChE, kemudian diprediksi bioavailabilitas dan toksisitas ligannya serta dianalisis interaksinya. Hasil penelitian menunjukkan galanthamine (ligan alami), donepezil, dan rivastigmine (ligan pembanding) memiliki nilai ΔG sebesar -10,5710, -10,3260, dan -7,3670 kkal/mol serta Ki sebesar 0,0175, 0,0265, dan 3,9261 μM, potensi inhibisi terbaik dimiliki oleh ligan fisetin dan morin dengan ΔG sebesar -10,4250 dan -10,3570 kkal/mol serta Ki sebesar 0,0224 dan 0,0251 μM. Kedua ligan memiliki nilai ΔG lebih negatif daripada ligan

pembanding dan berikatan dengan situs aktif secara kuat pada residu asam amino HIS447, sehingga dapat berpotensi sebagai inhibitor kompetitif enzim AChE serta bersifat mudah larut dan tidak toksik bagi tubuh.

***Kata kunci**: demensia; inhibitor asetilkolinesterase, jahe merah*

1. INTRODUCTION

Dementia is a neurodegenerative disorder characterized by progressive damage to neuronal cells in the brain, leading to cognitive decline or neuronal cell death. This condition results in a decreased level of acetylcholine (ACh) in the brain, thereby impairing synaptic transmission and disrupting inter-neuronal communication (DelAguila *et al*., 2015). Clinically, dementia manifests as impairments in memory, recall, thinking ability, learning capacity, and language function (Fitri *et al*., 2020). In 2019, dementia ranked as the seventh leading cause of death worldwide (WHO, 2020). Globally, the number of individuals affected by dementia is projected to triple from approximately 50 million to 152 million between 2017 and 2050 (WHO, 2017). In Indonesia, the prevalence is estimated to increase from 1.20 million to 3.98 million individuals over the period 2015–2050. This disease predominantly affects individuals aged over 65 years (Gultom *et al*., 2021).

Acetylcholine (ACh) is a key neurotransmitter responsible for memory signal transmission in the brain. However, the enzyme acetylcholinesterase (AChE) hydrolyzes ACh into acetic acid and choline. Continuous degradation of ACh by AChE contributes to cognitive impairment, highlighting the therapeutic need for AChE inhibitors (Dvir et al., 2010). Several pharmacological agents approved by the U.S. Food and Drug Administration (FDA), including donepezil, galantamine, and rivastigmine, act as AChE inhibitors for the treatment of dementia. Nevertheless, these drugs are not suitable for long-term use due to their high cost and the risk of adverse side effects (Tuzimski & Petruczynik, 2022). This limitation underscores the need for alternative therapeutic approaches derived from herbal sources that are safer and associated with fewer side effects.

Numerous studies have explored plant-derived bioactive compounds as potential treatments for dementia. Medicinal plants reported to enhance cognitive and memory functions include red betel leaf (*Piper crocatum*) (Syifa, 2021), ginger (*Zingiber officinale*) (Oboh *et al*., 2012), and fig fruit (*Ficus carica*) (Loizzo *et al*., 2014).

Ginger contains bioactive compounds such as alkaloids, tannins, flavonoids, and terpenoids, which have been demonstrated to exhibit acetylcholinesterase inhibitory activity, thereby slowing the degradation of ACh in the brain (Oboh *et al.,* 2012). Zhang et al. (2022) further reported that red ginger contains vanilloids, terpenes, flavonoids, phenolic compounds, alkaloids, tannins, organic acids, and amino acids, suggesting its potential as an AChE inhibitor. Red ginger has been widely used as a traditional herbal remedy due to its safety, effectiveness, and high therapeutic value. Compared to other ginger varieties, red ginger is more commonly utilized for medicinal purposes because of its higher essential oil content (2.58–3.72%) and oleoresin concentration (3%), which contribute to its enhanced pharmacological potency. Additionally, red ginger contains higher levels of phenolic and flavonoid compounds, including gingerol, zingerol, shogaol, gingerin, and zingiberene (Aryanta, 2019). Red ginger is abundant in Indonesia and is extensively used in herbal medicine. A study by Oboh *et al.* (2012) demonstrated that aqueous extracts of red ginger exhibited AChE inhibitory activity at concentrations ranging from 0 to 6.76 mg/mL, with an IC_{50} value of 3.030 mg/mL.

Previous in vivo studies have shown that ethanolic ginger extract significantly improves cognitive performance in rats, as indicated by reduced escape latency in the Morris water maze test at doses of 100–200 mg/kg (Wattanathorn *et al.,* 2011). While the acetylcholinesterase (AChE) inhibitory activity of red ginger has been reported in vitro, its molecular interactions with AChE have not yet been systematically investigated using in silico approaches. Therefore, this study aims to identify bioactive compounds from red ginger with potential AChE inhibitory activity as anti-dementia candidates using molecular docking analysis. Additionally, the study evaluates the bioavailability and toxicity profiles of selected ligands and elucidates key ligand–AChE interactions that may contribute to the inhibition of dementia progression.

2. MATERIALS AND METHODS

The equipment used in this study included a Biochemistry Laboratory computer (Biokimia 1401) equipped with an Intel® Core™ i9-9900 processor (3.60 GHz) and 32 GB RAM, as well as an ASUS X441M laptop powered by an Intel® Celeron® N4000 processor (1.10 GHz) with 4 GB RAM. Both systems operated on a 64-bit Windows 11 operating system. Molecular docking simulations were performed using YASARA Structure, Discovery Studio Visualizer, and PyMOL software packages.

The materials used in this study comprised the three-dimensional (3D) structure of the human acetylcholinesterase enzyme receptor (PDB ID: 4EY6), which was obtained from the RCSB Protein Data Bank in .pdb format (Cheung et al., 2012). A total of 163 bioactive compounds derived from red ginger were employed as test ligands, with their 3D structures downloaded from the PubChem database in .sdf format. Additionally, the corresponding SMILES representations of the ligands were retrieved from PubChem for further computational analysis.

Receptor and Ligand Preparation

The receptor used in this study was the human acetylcholinesterase enzyme with PDB ID 4EY6. Its three-dimensional (3D) structure was downloaded from the RCSB Protein Data Bank (https://www.rcsb.org/pdb/). The selected protein met key quality criteria, including a crystallographic resolution of less than 2.5 Å, structural stability, and the absence of mutations.

Protein preparation was performed using YASARA Structure. The 3D structure was imported, and all undesired residues and crystallographic water molecules were removed. The native ligand, galantamine (GNT), was separated from the receptor and saved as AC_ligand.* in .sdf, .yob, and .pdb formats. Hydrogen atoms were then added to the receptor, which was saved as AC_receptor.sce. Both the prepared receptor and the native ligand were also stored together in AC_preparation.sce format.

A total of 163 test ligands consisting of bioactive compounds from red ginger were employed, along with reference ligands (donepezil and rivastigmine) obtained based on literature reports from multiple journals. The three-dimensional structures of all ligands were downloaded from the PubChem database (https://pubchem.ncbi.nlm.nih.gov) in .sdf format. The ligands were imported into YASARA, subjected to energy minimization, and the prepared structures were saved in .pdb format.

Grid Box Validation

Validation was performed to determine the optimal grid box dimensions, define the receptor active site, and calculate the root mean square deviation (RMSD). The RMSD value was used to assess the appropriateness of the docking parameters and to compare

conformational changes of the native ligand before and after validation. Validation was conducted using 14 grid box sizes ranging from 0.5 to 7.0 Å, with 0.5 Å increments.

The prepared receptor was imported into YASARA, and the docking cube was adjusted to the different grid box sizes. The native ligand was removed and subsequently reintroduced during the redocking process. The receptor was treated as rigid and parameterized using the AMBER14 force field, then saved in AC_receptor.sce format. The ligand was docked into the receptor, and the resulting complex was saved as AC_complex.sce.

Grid box validation was executed by modifying the doc_run.mcr file to 999, followed by docking using the dock_run.mcr command. The validation output consisted of two files in .log and .yob formats. RMSD determination was carried out by loading the best validation result (.yob) together with the native ligand (.yob). The protein was removed, and both ligand structures were aligned to the same coordinates. RMSD values were then calculated using the RMSD of command. The optimal grid box size was selected based on the lowest Gibbs free energy (ΔG) value and an RMSD threshold of < 2 Å, which was subsequently used for molecular docking analysis.

Virtual Screening using YASARA

Virtual screening was performed by including the native ligand, two reference ligands, and 163 prepared test ligands, all of which were imported into YASARA. The ligands were merged into a single file and saved in AC_ligands.sdf format. The receptor corresponding to the optimal grid box was then loaded, and the combined ligand file was added to generate the complex, which was saved as AC_complexs.sce.

Virtual screening was conducted by setting the receptor as the target and executing the screening using the dock_runscreening command, configured to run 999 iterations. The screening outputs were generated in .log and .yob formats. The resulting binding poses were evaluated by comparing the Gibbs free energy (ΔG) values of the test ligands against those of the reference ligands.

Ligand Bioavailability Prediction

Bioavailability prediction analysis was performed by submitting the SMILES structures of the compounds, obtained from PubChem, to the Lipinski's Rule of Five web server (http://www.scfbio-iitd.res.in/software/drugdesign/lipinski.jsp). The analysis was conducted in accordance with Lipinski's Rule of Five criteria to evaluate the drug-likeness and oral bioavailability potential of the compounds.

Ligand Toxicity Prediction

Toxicity prediction analysis was conducted to assess the safety profile of the tested compounds in accordance with Lipinski-based drug-likeness considerations. Several key toxicity-related parameters were evaluated, including carcinogenicity, chronic oral toxicity, and Human Ether-à-go-go–Related Gene (hERG) inhibition. Toxicity predictions were performed by submitting the SMILES structures of the test ligands to the AdmetSAR platform (http://lmmd.ecust.edu.cn/admetsar2) and the pkCSM server (https://biosig.lab.uq.edu.au/pkcsm/).

Molecular Docking

Molecular docking was performed on the top-ranked test ligands that successfully passed the bioavailability and toxicity prediction analyses as well as the virtual screening stage. Seven best-performing ligands were selected based on the virtual screening results. Each selected ligand was individually loaded into YASARA along with the receptor prepared using the optimal grid box configuration, and the resulting complexes

were saved in the AC_complex.sce format. Docking simulations were conducted separately for each ligand using the dock_run.mcr command, which was configured to run 999 iterations. The docking outputs were generated in *.log and *.yob file formats.

Analysis of Ligand-Receptor Interactions

Ligand–receptor interaction analysis was conducted using both two-dimensional (2D) and three-dimensional (3D) approaches. The 2D interaction analysis was performed to identify hydrogen bonding and hydrophobic interactions between the ligand and the receptor using Discovery Studio Visualizer. In contrast, 3D molecular interaction analysis and structural visualization were carried out using PyMOL.

3. RESULTS

Receptor and Ligand Preparation

The receptor used in this study was human acetylcholinesterase (AChE) with PDB ID 4EY6 and a crystallographic resolution of 2.40 Å, obtained from the Research Collaboratory for Structural Bioinformatics (RCSB). X-ray structure validation based on wwPDB metrics indicated an R_free value of 0.208, a clashscore of 3, Ramachandran outliers of 0, side-chain outliers of 1.3%, and RSRZ outliers of 0.9% (Cheung *et al.,* 2012) (Figure 1). Overall, this structure was classified as high quality, as all validation parameters were within the favorable (blue) regions. The prepared protein structure consisted of a receptor–ligand complex between human AChE and galanthamine as the native ligand. Galanthamine functions as a known inhibitor of the AChE enzyme.

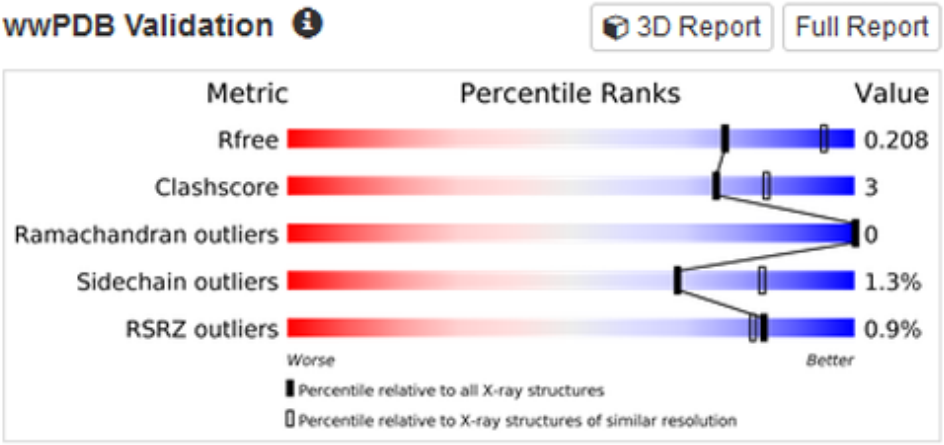

Figure 1. Validation of the X-ray crystal structure of acetylcholinesterase (AChE) (PDB ID: 4EY6).

A total of 163 test ligands derived from bioactive compounds identified in red ginger were used in this study, along with two reference ligands, donepezil and rivastigmine. These ligands were selected based on data compiled from published journal literature and were classified into several compound groups along with their respective counts (Table 1). Ligand preparation was performed through energy minimization, and the results confirmed that all ligands reached their lowest-energy conformations prior to molecular docking analyses.

Table 1. Classes and number of active compounds in red ginger (*Zingiber officinale* var. rubrum).

Class	Number	Source
Vanilloid	27	Zhang *et al.* 2022

Class	Number	Source
Monoterpene	41	Rinanda *et al*. 2018
Sesquiterpene	49	Rinanda *et al*. 2018
Diterpene	1	Zhang *et al.* 2022
Flavonoid	11	Zhang *et al.* 2022
Organic acids	13	Zhang *et al.* 2022
Amino Acids	8	Zhang *et al.* 2022
Other Compounds	13	Zhang *et al.* 2022
Total	163	

Grid Box Validation

The prepared acetylcholinesterase (AChE) protein was subjected to grid box validation to determine the optimal grid dimensions capable of accurately encompassing the active site of the target enzyme during molecular docking. The optimal grid box was selected based on two criteria: a root mean square deviation (RMSD) value of less than 2 Å and the lowest Gibbs free energy (ΔG) obtained from redocking analyses. The best grid box size was determined to be 7 Å, yielding the lowest RMSD value of 0.3856 Å and the most favorable binding free energy (ΔG) of −10.5710 kcal/mol, which was more negative than those obtained using other grid box sizes. The grid center was defined at coordinates X = 7.670, Y = −2.529, and Z = 123.929. Superposition of the redocked ligand with the crystallographic ligand demonstrated a high degree of structural overlap, indicating excellent docking accuracy (Figure 2).

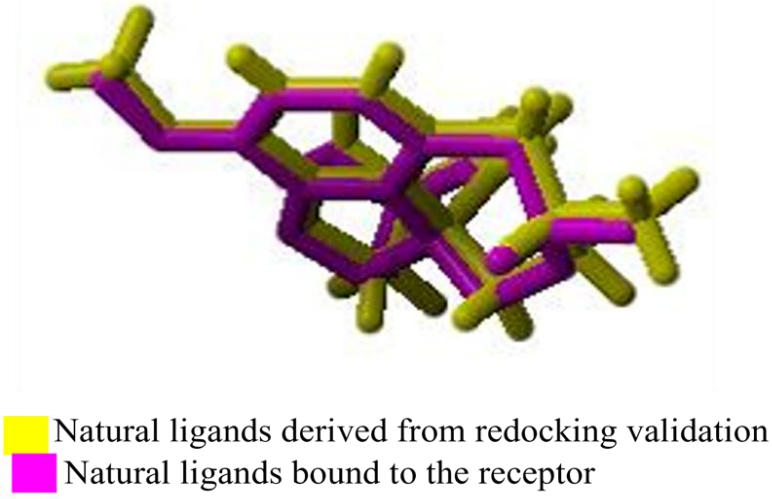

Figure 2. Validation of the grid box in YASARA.

Virtual Screening

Based on the study results, galanthamine (the native ligand) exhibited a binding free energy (ΔG) of −10.571 kcal/mol, whereas the reference ligands donepezil and rivastigmine showed ΔG values of −10.2890 and −7.4130 kcal/mol, respectively. Test ligands were considered to pass the screening stage if they exhibited ΔG values more negative than that of the reference ligand rivastigmine. An ideal ligand candidate is defined as one with a ΔG value comparable to that of the native ligand and the reference compounds (Putri et al., 2023). This criterion is further supported by the study of Baskaran et al. (2020), which reported that rivastigmine exhibits a relatively weak binding affinity with a ΔG value of only −3.3 kcal/mol; therefore, ligands with more negative ΔG values than rivastigmine are considered more favorable.

In total, 88 test ligands passed the screening stage, with Gibbs free energy (ΔG) values ranging from −10.928 to −7.4180 kcal/mol (Table 2). Based on an extensive

literature survey, 25 of these 88 screened ligands were identified as characteristic bioactive compounds of red ginger. The ligands that passed this stage were subsequently subjected to bioavailability and toxicity prediction analyses.

Table 2. Binding free energy and bioavailability analysis of active compounds from red ginger identified through virtual screening.

No.	Ligand name	Gibbs free energy (kcal/mol)	Molecular weight (Da)	Log P	H-bond donors	H-bond acceptors	Molar refractivity
	Galanthamine (natural ligand)	-10,5710	287	1,8503	1	4	79,8028
	Donepezil (positive control ligand)	-10,2890	379	4,1284	0	4	109,1975
	Rivastigmine (positive control ligand)	-7,4130	250	2,7597	0	4	72,8720
1.	*Myricetin*	-10,9280	318	1,7165	6	8	75,7153
2.	*Quercetin*	-10,6370	302	2,0109	5	7	74,0505
3.	Fisetin	-10,4140	286	2,3053	4	6	72,3857
4.	Morin	-10,3600	302	2,0109	5	7	74,0505
5.	Kaempferol	-10,2360	286	2,3053	4	6	72,3857
6.	Naringenin	-10,1740	272	2,5099	3	5	70,1949
7.	*(+)- Catechin*	-10,0340	290	1,2987	5	6	71,6430
8.	*(−)-Epicatechin*	-9,8860	290	1,2987	5	6	71,6430
9.	*Hexahydro-curcumin*	-9,6660	374	0,0000	3	6	0,0000
10.	Apigenin	-9,5070	270	2,4196	3	5	70,8139
11.	*(2R,4S,5R)-2-(Acetoxymethyl)-6-(2-methoxy-4-((E)-3-oxodec-4-en-1-yl)phenoxy)tetrahydro-2H-pyran-3,4,5-triyl triacetate*	-9,4460	606	0,2704	0	12	141,6151
12.	*[8]-Gingerdiol 3R,5S-diacetate*	-9,1810	408	-1,2025	1	6	87,2788
13.	*[8]-Gingerdiol 3S,5S-diacetate*	-9,1810	408	1,0419	1	6	99,9878
14.	*[10]-Gingerdiol 3R,5S-diacetate*	-9,1000	436	-1,0399	1	6	93,7648
15.	*[10]-Gingerdiol 3S,5S-diacetate*	-9,1000	436	1,2045	1	6	106,4738
16.	*[6]-Gingerdiol 3R,5S-diacetate*	-9,0280	380	-1,2684	1	6	80,6498
17.	*[6]-Gingerdiol 3S,5S-diacetate*	-9,0280	380	0,8794	1	6	935018
18.	*3,5-Diacetoxy-1-(4-hydroxy-3-methoxyphenyl)decane*	-9,0260	380	-1,2684	1	6	80,6498
19.	8-Shogaol	-8,9940	304	2,4439	1	3	75,6018
20.	*(E)-1-(3-Methoxy-4-(((3R,4S,6R)-3,4,5-trihydroxy-6-(hydroxymethyl)tetrahydro-2H-pyran-2-yl)oxy)phenyl)dec-4-en-3-one*	-8,9330	438	-0,2068	4	8	100,2222
21.	10-Shogaol	-8,8430	332	2,6065	1	3	82,0878
22.	Rutin	-8,6550	610	-1,9854	10	16	133,9525
23.	6-Shogaol	-8,6330	276	2,2813	1	3	69,1158

No.	Ligand name	Gibbs free energy (kcal/mol)	Molecular weight (Da)	Log P	H-bond donors	H-bond acceptors	Molar refractivity
24.	*Flavylium*	-8,6210	208	3,8335	0	1	65,2870
25.	*5-Hydroxy-1-(3-methoxy-4-(((3R,4S,6R)-3,4,5-trihydroxy-6-(hydroxymethyl)tetrahydro-2H-pyran-2-yl)oxy)phenyl)decan-3-one*	-8,5890	456	0,0000	5	9	0,0000
26.	*4-Gingeracetate*	-8,5540	352	0,2099	1	6	77,4288
27.	10-Gingerol	-8,4970	350	0,0000	2	4	0,0000
28.	*1-Dehydro-6-gingerdione*	-8,4640	290	0,0000	1	4	0,0000
29.	8-Gingerol	-8,4260	322	0,0000	2	4	0,0000
30.	*β-Atlantone*	-8,4220	214	1,8333	0	1	58,5405
31.	(3R,5S)-[10]-Gingerdiol	-8,3510	352	0,9659	3	4	85,7774
32.	(3S,5S)-[10]-Gingerdiol	-8,3510	352	0,9659	3	4	85,7774
33.	*(2R,4S,5R)-2-(Acetoxymethyl)-6-(4-(5-hydroxy-3-oxodecyl)-2-methoxyphenoxy)tetrahydro-2H-pyran-3,4,5-triyl triacetate*	-8,2580	624	0,0000	1	13	0,0000
34.	*6-Dehydro-gingerdione*	-8,2540	290	2,6696	2	4	74,1336
35.	6-Gingerol	-8,2540	294	0,0000	2	4	0,0000
36.	*5-Methoxy-1-(4-hydroxy-3-methoxyphenyl)-3-decanone*	-8,2530	308	0,0000	1	4	0,0000
37.	*β-Cubebene*	-8,2430	204	0,0000	0	0	0,0000
38.	*β-Elemene*	-8,2430	204	1,4913	0	0	51,9150
39.	*γ-Eudesmol*	-8,2240	222	0,0673	1	1	56,2708
40.	*5-Methoxy-1-(4-hydroxy-3-methoxyphenyl)-3-tetradecanone:*	-8,2230	364	0,0000	1	4	0,0000
41.	*Histidine*	-8,2190	155	-1,6637	0	5	31,7370
42.	(3S,5S)-[8]-Gingerdiol	-8,2010	324	0,8034	3	4	79,2914
43.	*α-Selinene*	-8,1970	204	1,8342	0	0	54,5550
44.	*3-Hydroxy-1-(4-hydroxy-3-methoxyphenyl)-5-decanone*	-8,1840	294	1,0082	2	4	70,5156
45.	*Cyclosativene*	-8,1810	204	1,3917	0	0	52,2270
46.	*δ-Cadinene*	-8,1810	204	1,6288	0	0	55,5570
47.	*δ-Elemene*	-8,1810	202	2,2220	0	0	55,2710
48.	*β-Caryophyllene*	-8,1580	206	1,2304	0	0	53,8330
49.	*Germacrene B*	-8,1470	204	0,0000	0	0	0,0000
50.	*Germacrene D*	-8,1470	206	0,0000	0	0	0,0000
51.	(3R,5S)-[8]-Gingerdiol	-8,1430	324	0,8034	3	4	79,2914
52.	(3R,5S)-[6]-Gingerdiol	-8,1170	296	-1,5070	3	4	59,9534
53.	*Cedr-8-ene*	-8,0790	204	1,1491	0	0	53,0230
54.	*Cedrene*	-8,0790	204	1,1491	0	0	53,0230
55.	*α-Caryophyllene*	-8,0110	208	1,3896	0	0	52,5430
56.	*α-Copaene*	-8,0110	204	1,4730	0	0	53,0370
57.	*α-Curcumene*	-8,0110	202	1,6572	0	0	59,0280

No.	Ligand name	Gibbs free energy (kcal/mol)	Molecular weight (Da)	Log P	H-bond donors	H-bond acceptors	Molar refractivity
58.	*α-Farnesene*	-8,0110	204	0,0000	0	0	0,0000
59.	*α-Humulene*	-8,0110	208	1,3896	0	0	52,5430
60.	*α-Muurolene*	-8,0110	204	1,7370	0	0	54,9090
61.	*α-Panasinsen*	-8,0110	204	0,9844	0	0	51,7190
62.	*α-trans-Bergamotene*	-7,9820	204	0,6724	0	0	53,4970
63.	Farnesal	-7,9600	220	0,0000	0	1	0,0000
64.	*Caryophyllenol*	-7,9570	220	0,5610	1	1	55,9548
65.	(3S,5S)-[6]-Gingerdiol	-7,9490	296	0,6408	3	4	72,8054
66.	*β-Eudesmol*	-7,9450	220	1,0746	1	1	56,3618
67.	*Allo-aromadendrene*	-7,9040	204	1,3648	0	0	53,6850
68.	*β-Bisabolene*	-7,8440	200	2,3117	0	0	56,0900
69.	*1-(4-Hydroxy-3-methoxyphenyl)-3,5-decanediol*	-7,8170	296	-1,5070	3	4	59,9534
70.	*Zingiberene*	-7,7970	204	0,9881	0	0	58,2510
71.	*β-Bisabolol*	-7,7960	218	0,4590	1	1	59,7478
72.	*Cubenol*	-7,7580	224	0,5100	1	1	56,5968
73.	*β-Cedren-9-α-ol*	-7,6980	220	0,9633	1	1	53,7058
74.	*β-Sesquiphellandrene*	-7,6600	204	1,1473	0	0	56,9610
75.	*Bisabolene*	-7,6600	200	0,0000	0	0	0,0000
76.	*4-(1,5-Dimethylhex-4-enyl)cyclohex-2-enone*	-7,6460	204	0,8245	0	1	57,0790
77.	*Spathulenol*	-7,6160	222	0,6338	1	1	55,4888
78.	*τ-Eudesmol*	-7,6160	222	1,0628	1	1	57,9608
79.	*τ-Muurolol*	-7,6160	220	1,5595	1	1	59,5168
80.	*cis-nerolidol*	-7,6140	222	0,0000	1	1	0,0000
81.	*α-Bisabolol*	-7,5950	218	0,6641	1	1	59,4498
82.	*α-Cadinol*	-7,5950	222	0,8978	1	1	57,3608
83.	*Elemol*	-7,5550	224	0,7606	1	1	53,0628
84.	*epi-Globulol*	-7,5550	222	0,6338	1	1	55,4888
85.	*trans-nerolidol*	-7,5010	222	0,0000	1	1	0,0000
86.	*Phytol*	-7,4950	296	0,9241	1	1	76,4668
87.	*Caryophyllene oxide*	-7,4700	220	0,9118	0	1	52,0590
88.	*Ethyl cinnamate*	-7,4180	176	1,8699	0	2	48,0540

Ligand Bioavailability Prediction

A total of 88 screened ligands, along with the native ligand and two reference compounds, were subsequently evaluated for their bioavailability characteristics. The analysis was conducted in accordance with Lipinski's Rule of Five, which includes the following criteria: molecular weight < 500 Da, logP < 5, hydrogen bond donors < 5, hydrogen bond acceptors < 10, and molar refractivity within the range of 40–130 (Lipinski et al., 2012). Ligands violating more than two of Lipinski's criteria were considered unsuitable as drug candidates due to poor predicted oral bioavailability.

The results demonstrated that 85 test ligands satisfied the bioavailability criteria, whereas ligands numbered 11, 22, and 33 failed to meet the Lipinski requirements and were therefore excluded from further consideration (Table 2).

Ligand Toxicity Prediction

The 85 ligands that passed the bioavailability assessment were subsequently subjected to toxicity prediction. The evaluated parameters included hERG inhibition, carcinogenicity, chronic oral toxicity, and acute oral toxicity. The hERG analysis indicated that all ligands met the safety threshold; however, one compound was classified as a strong hERG inhibitor, namely donepezil, which served as the reference ligand in this study. Among the tested compounds, ligands 4 and 5 exhibited the highest predicted inhibition values (0.9795), whereas donepezil showed the lowest inhibition value (0.5386). Carcinogenicity prediction revealed that three compounds—ligands 55, 60, and 85—were excluded as drug candidates due to their carcinogenic potential. The highest carcinogenicity score was observed for ligand 19 (0.9606), while the lowest score was recorded for ligand 85 (0.5070).

Table 3. Ligand Toxicity Prediction.

No.	Ligand name	hERG inhibition		Carcinogenicity		Chronic oral toxicity		Acute oral toxicity	
		Category	Score	Category	Score	Category	Score	Category	Score
	Galanthamine (natural ligand)	IL	0,802	NK	0,905	NT	0,966	III	0,494
	Donepezil (positive control ligand)	IK	0,538	NK	0,952	NT	0,991	III	0,525
	Rivastigmine (positive control ligand)	IL	0,935	NK	0,585	NT	11,630	II	0,667
1	*Myricetin*	IL	0,978	NK	0,945	NT	27,180	II	0,734
2	*Quercetin*	IL	0,978	NK	0,945	NT	26,120	II	0,734
3	Fisetin	IL	0,977	NK	0,939	NT	19,210	II	0,718
4	Morin	IL	0,979	NK	0,936	NT	24,480	II	0,623
5	Kaempferol	IL	0,979	NK	0,936	NT	25,050	II	0,623
6	Naringenin	IL	0,964	NK	0,936	NT	19,440	II	0,368
7	*(+)- Catechin*	IL	0,966	NK	0,953	NT	2,500	IV	0,643
8	*(−)-Epicatechin*	IL	0,966	NK	0,953	NT	2,500	IV	0,643
9	*Hexahydro-curcumin*	IL	0,903	NK	0,930	NT	22,380	III	0,662
10	Apigenin	IL	0,955	NK	0,918	NT	22,980	III	0,701
11	*[8]Gingerdiol 3R,5S-diacetate*	IL	0,905	NK	0,864	NT	17,690	III	0,620
12	*[8]Gingerdiol 3S,5S-diacetate*	IL	0,905	NK	0,864	NT	17,690	III	0,620
13	*[10]Gingerdiol 3R,5S-diacetate*	IL	0,905	NK	0,864	NT	17,120	III	0,620
14	*[10]Gingerdiol 3S,5S-diacetate*	IL	0,905	NK	0,864	NT	17,120	III	0,620

No.	Ligand name	hERG inhibition		Carcinogenicity		Chronic oral toxicity		Acute oral toxicity	
		Category	Score	Category	Score	Category	Score	Category	Score
15	*[6]Gingerdiol 3R,5S-diacetate*	IL	0,905	NK	0,864	NT	18,370	III	0,620
16	*[6]Gingerdiol 3S,5S-diacetate*	IL	0,905	NK	0,864	NT	1,837	III	0,620
17	*3,5-Diacetoxy-1-(4-hydroxy-3-methoxyphenyl)decane*	IL	0,905	NK	0,864	NT	13,230	III	0,620
18	8-Shogaol	IL	0,864	NK	0,878	NT	22,390	III	0,691
19	*(E)-1-(3-Methoxy-4-(((3R,4S,6R)-3,4,5-trihydroxy-6-(hydroxymethyl)tetrahydro-2H-pyran-2-yl)oxy)phenyl)dec-4-en-3-one*	IL	0,926	NK	0,960	NT	39,530	III	0,605
20	10-Shogaol	IL	0,864	NK	0,878	NT	23,210	III	0,691
21	6-Shogaol	IL	0,864	NK	0,878	NT	21,590	III	0,691
22	*Flavylium*	IL	0,915	NK	0,847	NT	11,180	III	0,764
23	*5-Hydroxy-1-(3-methoxy-4-(((3R,4S,6R)-3,4,5-trihydroxy-6-(hydroxymethyl)tetrahydro-2H-pyran-2-yl)oxy)phenyl)decan-3-one*	IL	0,949	NK	0,957	NT	39,120	III	0,620
24	*4-Gingeracetate*	IL	0,883	NK	0,862	NT	18,510	III	0,640
25	10-Gingerol	IL	0,940	NK	0,912	NT	17,830	III	0,600
26	*1-Dehydro-6-gingerdione*	IL	0,848	NK	0,886	NT	19,370	III	0,640
27	8-Gingerol	IL	0,940	NK	0,912	NT	17,020	III	0,600
28	*β-Atlantone*	IL	0,641	NK	0,656	NT	11,350	III	0,827
29	(3R,5S)-[10]-Gingerdiol	IL	0,900	NK	0,915	NT	27,760	III	0,689
30	(3S,5S)-[10]-Gingerdiol	IL	0,900	NK	0,915	NT	27,760	III	0,689
31	*6-Dehydro-gingerdione*	IL	0,900	NK	0,898	NT	15,390	III	0,570
32	6-Gingerol	IL	0,940	NK	0,912	NT	16,310	III	0,600
33	*5-Methoxy-1-(4-hydroxy-3-methoxyphenyl)-3-decanone*	IL	0,888	NK	0,845	NT	17,710	III	0,713
34	*β-Cubebene*	IL	0,959	NK	0,816	NT	14,060	III	0,827
35	*β-Elemene*	IL	0,837	NK	0,682	NT	13,090	III	0,819
36	*γ-Eudesmol*	IL	0,883	NK	0,850	NT	12,490	IV	0,481
37	*5-Methoxy-1-(4-hydroxy-3-methoxyphenyl)-3-tetradecanone:*	IL	0,888	NK	0,845	NT	19,230	III	0,713
38	*Histidine*	IL	0,989	NK	0,920	NT	18,060	III	0,584

No.	Ligand name	hERG inhibition		Carcinogenicity		Chronic oral toxicity		Acute oral toxicity	
		Category	Score	Category	Score	Category	Score	Category	Score
39	(3S,5S)-[8]-Gingerdiol	IL	0,900	NK	0,915	NT	26,230	III	0,689
40	*α-Selinene*	IL	0,862	NK	0,780	NT	13,510	III	0,846
41	*3-Hydroxy-1-(4-hydroxy-3-methoxyphenyl)-5-decanone*	IL	0,940	NK	0,912	NT	15,810	III	0,600
42	*Cyclosativene*	IL	0,974	NK	0,799	NT	13,660	III	0,489
43	*δ-Cadinene*	IL	0,808	NK	0,804	NT	14,480	III	0,713
44	*δ-Elemene*	IL	0,936	NK	0,652	NT	13,590	III	0,904
45	*β-Caryophyllene*	IL	0,922	NK	0,686	NT	14,160	III	0,820
46	*Germacrene B*	IL	0,837	NK	0,642	NT	14,160	III	0,742
47	*Germacrene D*	IL	0,837	NK	0,628	NT	14,130	III	0,814
48	(3R,5S)-[8]-Gingerdiol	IL	0,900	NK	0,915	NT	26,230	III	0,689
49	(3R,5S)-[6]-Gingerdiol	IL	0,900	NK	0,915	NT	15,590	III	0,689
50	*Cedr-8-ene*	IL	0,943	NK	0,814	NT	13,990	III	0,753
51	*Cedrene*	IL	0,943	NK	0,814	NT	13,990	III	0,753
52	*α-Caryophyllene*	IL	0,916	NK	0,653	NT	13,360	III	0,688
53	*α-Copaene*	IL	0,912	NK	0,783	NT	13,560	III	0,776
54	*α-Curcumene*	IL	0,818	NK	0,645	NT	12,970	III	0,934
55	*α-Farnesene*	IL	0,769	K	0,569	NT	13,670	III	0,907
56	*α-Humulene*	IL	0,916	NK	0,653	NT	13,360	III	0,688
57	*α-Muurolene*	IL	0,850	NK	0,771	NT	13,820	III	0,683
58	*α-Panasinsen*	IL	0,950	NK	0,808	NT	13,540	III	0,779
59	*α-trans-Bergamotene*	IL	0,870	NK	0,735	NT	13,670	III	0,853
60	Farnesal	IL	0,779	K	0,544	NT	12,250	III	0,737
61	*Caryophyllenol*	IL	0,869	NK	0,867	NT	14,810	III	0,802
62	(3S,5S)-[6]-Gingerdiol	IL	0,900	NK	0,915	NT	24,840	III	0,689
63	*β-Eudesmol*	IL	0,883	NK	0,827	NT	13,040	III	0,652
64	*Allo-aromadendrene*	IL	0,964	NK	0,746	NT	13,320	III	0,838
65	*β-Bisabolene*	IL	0,732	NK	0,651	NT	13,470	III	0,908
66	*1-(4-Hydroxy-3-methoxyphenyl)-3,5-decanediol*	IL	0,900	NK	0,915	NT	15,590	III	0,689
67	*Zingiberene*	IL	0,732	NK	0,662	NT	13,290	III	0,861
68	*β-Bisabolol*	IL	0,815	NK	0,859	NT	12,020	III	0,872
69	*Cubenol*	IL	0,835	NK	0,916	NT	13,090	III	0,850
70	*β-Cedren-9-α-ol*	IL	0,890	NK	0,902	NT	12,000	III	0,819
71	*β-Sesquiphellandrene*	IL	0,732	NK	0,651	NT	13,140	III	0,908
72	*Bisabolene*	IL	0,732	NK	0,662	NT	13,760	III	0,861
73	*4-(1,5-Dimethylhex-4-enyl)cyclohex-2-enone*	IL	0,617	NK	0,807	NT	11,940	III	0,568

No.	Ligand name	hERG inhibition		Carcinogenicity		Chronic oral toxicity		Acute oral toxicity	
		Category	Score	Category	Score	Category	Score	Category	Score
74	*Spathulenol*	IL	0,952	NK	0,882	NT	11,680	III	0,764
75	*τ-Eudesmol*	IL	0,914	NK	0,880	NT	15,310	III	0,864
76	*τ-Muurolol*	IL	0,870	NK	0,909	NT	14,750	III	0,851
77	*cis-nerolidol*	IL	0,846	NK	0,583	NT	11,870	III	0,900
78	*α-Bisabolol*	IL	0,831	NK	0,773	NT	11,780	III	0,848
79	*α-Cadinol*	IL	0,870	NK	0,909	NT	14,750	III	0,851
80	*Elemol*	IL	0,860	NK	0,752	NT	12,290	III	0,607
81	*epi-Globulol*	IL	0,977	NK	0,849	NT	11,870	III	0,764
82	*trans-nerolidol*	IL	0,846	NK	0,583	NT	11,870	III	0,900
83	*Phytol*	IL	0,783	NK	0,505	NT	12,320	III	0,855
84	*Caryophyllene oxide*	IL	0,872	NK	0,729	NT	11,930	III	0,816
85	*Ethyl cinnamate*	IL	0,944	K	0,507	NT	20,140	III	0,962

Notes = indicates that the ligand is **toxic**; **IL** = weak inhibitor; **IK** = strong inhibitor; **NK** = non-carcinogenic; **K** = carcinogenic; **NT** = no observed chronic toxic effects.

Molecular Docking, Gibbs Free Energy, Inhibition Constant

Test ligands that passed both bioavailability and toxicity predictions were subsequently subjected to molecular docking for validation. Based on this study, the natural ligand galanthamine exhibited a Gibbs free energy (ΔG) value of −10.5710 kcal/mol, while the reference ligands donepezil and rivastigmine showed ΔG values of −10.3260 and −7.3670 kcal/mol, respectively.

From the ligands that passed the screening stage, seven top candidates were selected, consisting of five ligands with the most favorable ΔG values and two marker compounds of red ginger with ΔG values closest to that of the natural ligand. The selection of these seven ligands was based on their proximity to the ΔG value of the natural ligand, as ligands with similar ΔG values are considered to possess high binding affinity and therefore potential competitiveness with the natural ligand.

The ligands myricetin and quercetin exhibited the most favorable (more negative) ΔG values compared to both the natural and reference ligands. In contrast, fisetin and morin displayed negative ΔG values that were less favorable than the natural ligand but more favorable than the reference ligands. Kaempferol, [8]-gingerdiol 3R,5S-diacetate, and [10]-gingerdiol 3R,5S-diacetate showed negative ΔG values that were less favorable than those of both the natural ligand and the reference ligand donepezil (Table 4).

Among all tested ligands, myricetin demonstrated the most favorable binding affinity, with the lowest ΔG value of −10.9270 kcal/mol. Conversely, [10]-gingerdiol 3R,5S-diacetate exhibited the least favorable ΔG value among the selected ligands, at −9.2700 kcal/mol. The molecular docking results for the ten ligands were consistent with the virtual screening outcomes, as the ΔG values did not differ substantially between the two approaches.

Another important parameter evaluated in molecular docking analysis was the inhibition constant (Ki). The results indicated that myricetin possessed the lowest Ki value (0.0096 µM), suggesting the strongest inhibitory potential, whereas rivastigmine exhibited the highest Ki value (3.9261 µM), indicating the weakest inhibition among the tested compounds (Table 4).

Table 4. Molecular docking of the best-performing ligands.

No.	Ligand name	Gibbs free energy (kcal/mol)	Inhibition constant (µM)
	Galanthamine (natural ligand)	-10,5710	0,0175
	Donepezil (positive control ligand)	-10,3260	0,0265
	Rivastigmine positive control ligand)	-7,3670	3,9261
1.	*Myricetin*	-10,9270	0,0096
2.	*Quercetin*	-10,6420	0,0155
3.	Fisetin	-10,4250	0,0224
4.	Morin	-10,3570	0,0251
5.	Kaempferol	-10,2510	0,0300
6.	*[8]-Gingerdiol 3R,5S-diacetate*	-9,4080	0,1248
7.	*[10]-Gingerdiol 3R,5S-diacetate*	-9,2700	0,1576

Important Residual Interactions

The molecular docking results were subsequently visualized in two dimensions (2D) using Discovery Studio Visualizer and in three dimensions (3D) using PyMOL. Visualization was also performed for the natural ligand and the reference ligands. Based on the results, the 2D visualization revealed multiple interactions between the ligands and amino acid residues of the AChE enzyme, including van der Waals interactions, hydrophobic interactions, hydrogen bonds, as well as unfavorable donor–donor interactions. The natural ligand galanthamine interacted with several amino acid residues through various types of interactions (Figure 3).

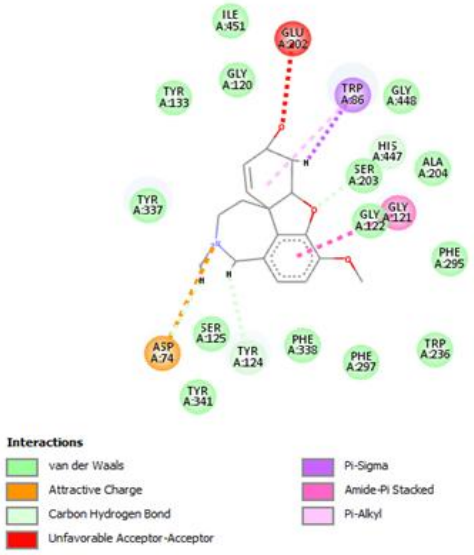

Figure 3. Two-dimensional visualization of the molecular docking of the natural ligand galanthamine.

Based on the results, all ligands formed hydrogen bond interactions; however, fisetin exhibited the highest number of hydrogen bonds compared with the other ligands. This ligand also showed strong interactions with the amino acid residues HIS447 and ASP72. The next highest number of hydrogen bonds was observed for quercetin, which displayed strong interactions with ASN87, followed by morin with TYR72 and kaempferol with HIS447.

All ligands also formed hydrophobic and van der Waals interactions with 12 to 25 amino acid residues of the AChE enzyme. However, these interactions mainly function as stabilizing forces and are more easily disrupted compared with hydrogen bonds. Myricetin and [8]-gingerdiol 3R,5S-diacetate exhibited unfavorable interactions, indicating the presence of unstable contacts at residues ASP74 and SER203 (Table 5).

Table 5. Amino acid residues involved in molecular docking interactions.

Ligand name	Residues involved in molecular docking interactions			
	Hydrogen bonds	**Hydrophobic interactions**	**van der Waals bonds**	**Unfavorable interactions**
Galanthamine (natural ligand)	HIS447 (2,56 Å), ASP74 (2,95 Å), TYR124 (2,40 Å)	TRP86, GLY121	SER203, TYR341, ALA204, GLY120, GLY122, GLY448, ILE451, PHE295, PHE297, PHE338, SER125, TRP236, TYR133, TYR337	GLU202
Donepezil (positive control ligand)	TYR124 (2,45 Å)	TRP286, GLY120	HIS447, SER203, TYR72, TYR341, ALA127, ARG296, GLY121, GLY122, GLY126, GLU202, GLU292, LEU130, LEU289, TYR133, TYR119, PHE295, PHE297, PHE338, SER125, SER293, TYR337, TRP86, VAL294	
Rivastigmine positive control ligand)	SER203 (2,74 Å), ASP74 (2,66 Å), TYR124 (2,78 Å), GLY121(2,36 Å), GLY122 (2,97 Å)	HIS447, PHE338,PHE297	TYR341, ALA204, ASN87, GLY120, GLY126, LEU130, SER125, TRP86, THR83, TYR133, TYR337	
Myricetin	HIS447 (2,33 Å), ASN87 (2,19 Å), GLY121(2,91 Å), SER125 (2,42 Å)	TRP86, TYR337	TYR72, TYR124, GLN71, GLY126, LEU130, GLY120, GLU202, GLY448, ILE451, PRO88, TYR449, TYR133, VAL73	ASP74
Rivastigmine positive control ligand)	SER203 (2,74 Å), ASP74 (2,66 Å), TYR124 (2,78 Å), GLY121(2,36 Å), GLY122 (2,97 Å)	HIS447, PHE338,PHE297	TYR341, ALA204, ASN87, GLY120, GLY126, LEU130, SER125, TRP86, THR83, TYR133, TYR337	
Myricetin	HIS447 (2,33 Å), ASN87 (2,19 Å), GLY121(2,91 Å), SER125 (2,42 Å)	TRP86, TYR337	TYR72, TYR124, GLN71, GLY126, LEU130, GLY120, GLU202, GLY448, ILE451, PRO88, TYR449, TYR133, VAL73	ASP74
Quercetin	ASP74 (2,42 Å), ASN87 (1,97 Å), GLU202 (2,38 Å), SER125 (2,53 Å), VAL73 (2,96 Å)	TRP86, TYR337	HIS447, SER203, TYR72, TYR124, GLN71, GLY121, GLY120, GLY126, GLY448, ILE451, PRO88, TYR133, TYR449	
Fisetin	HIS447 (1,87 Å), ASP74 (2,12 Å), TYR72 (3,07 Å), ASN87 (2,26 Å), GLY121 (2,86 Å), SER125 (2,54 Å), VAL73 (2,96 Å),	TRP86, TYR337	TYR124, GLN71, GLY120, GLY126, GLU202, GLY448, LEU130, PRO88, TYR133, TYR449	
Morin	HIS447 (2,35 Å), ASP74 (2,42 Å), TYR72 (1,73 Å), GLY120 (2,88 Å), SER125 (2,58 Å)	TRP86, TYR337	TYR124, ASN87, GLY121, GLY126, GLY448, GLU202, ILE451, TYR133, GLN71, PRO88, TYR449, VAL73	

Ligand name	Residues involved in molecular docking interactions			
	Hydrogen bonds	**Hydrophobic interactions**	**van der Waals bonds**	**Unfavorable interactions**
Kaempferol	HIS447 (2,20 Å), GLY121 (2,92 Å), ASP74 (2,41 Å), VAL73 (2,95 Å), SER125 (2,55 Å),	TRP86, TYR337	TYR72, TYR124, ASN87, GLN71, GLY120, GLY126, GLU202, GLY448, ILE451, PRO88, TYR133, TYR449	SER203
[8]-Gingerdiol 3R,5S-diacetate	HIS447 (2,87 Å), GLU202 (1,91 Å), GLY448 (2,74 Å), SER125 (2,12 Å),	,TYR341, TRP86, PHE338, VAL294	ASP74, TYR72, TYR124, TRP286, ALA204, ARG296, GLY120, GLY121, GLY 122, ILE451, PHE295, PHE297, TYR133, SER293, TYR337, TYR449, VAL73	
[10]-Gingerdiol 3R,5S-diacetate	SER125 (2,16 Å)	TYR341, TRP286, TRP86	HIS447, SER203, ASP74, TYR72, TYR124, ALA204, ARG296, GLY120, GLY121, GLY122, GLU202, GLU448, ILE451, PHE338, PHE295, PHE297, VAL294, SER293, TYR119, TYR133, TYR337, TYR449	

The results demonstrated that all ligands interacted with the key binding sites, namely the catalytic anionic site (CAS) and the peripheral anionic site (PAS). Quercetin, [8]-gingerdiol 3R,5S-diacetate, and [10]-gingerdiol 3R,5S-diacetate exhibited multiple interactions with these key sites; however, the binding affinities were relatively weak. In contrast, fisetin showed strong binding to the CAS at residue HIS447 and to the PAS at residues ASP74 and TYR72.

Morin also exhibited strong interactions with the PAS at residues TYR72 and TYR125, as well as with the CAS at HIS447. These two ligands demonstrated the highest number of strong interactions at critical residues and possessed ΔG values close to that of the natural ligand and lower than those of the reference ligands. Three-dimensional visualization using PyMOL revealed that galanthamine binds within the enzyme pocket region (Figure 4).

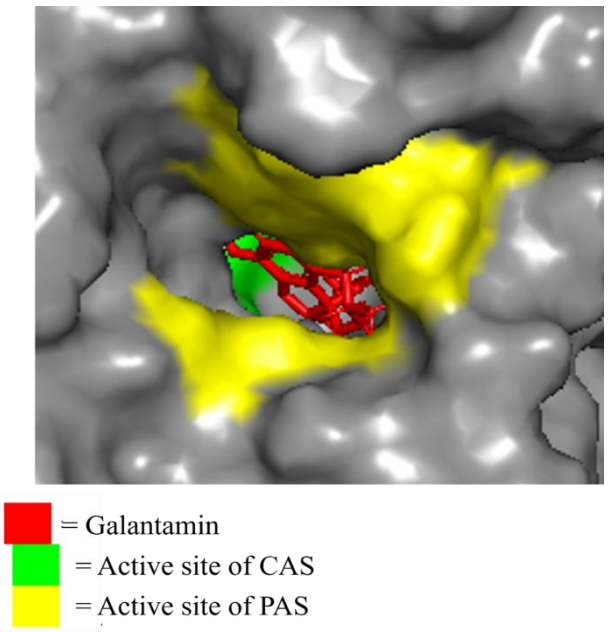

Figure 4. Three-dimensional visualization of the molecular docking of the natural ligand galanthamine.

4. DISCUSSION

Receptor and ligand preparation

The receptor used in this study was acetylcholinesterase (AChE) with PDB ID 4EY6, which has a crystal structure resolution of 2.40 Å. Protein structures with a crystal

resolution below 2.50 Å are considered to represent high-quality protein–ligand complexes and are suitable for molecular docking studies (Greenidge *et al.,* 2013). Structural validation of the AChE receptor based on wwPDB analysis indicated favorable quality parameters, including Rfree, clashscore, Ramachandran outliers, side-chain outliers, and RSRZ, all of which fell within the acceptable (blue) regions (Smart *et al*., 2018).

The Rfree value reflects the agreement between observed and calculated structure factor amplitudes. Ramachandran outliers represent the percentage of residues deviating from favored backbone conformations, while clashscore indicates the number of steric overlaps between atom pairs within the model. Side-chain outliers denote the proportion of residues with unusual side-chain conformations, and RSRZ evaluates the local real-space agreement between individual residues and the experimental data (Smart *et al.,* 2018).

Receptor preparation resulted in a structure consisting of chain A, which was saved in .sce format, while ligands were saved in .pdb format. Preparation involved the removal of non-essential residues and crystallographic water molecules, as well as the addition of hydrogen atoms. The removal of water molecules and undesired residues was performed to prevent interference during the docking process, ensuring that only receptor–ligand interactions were evaluated (Greenidge *et al.,* 2013). The natural ligand galanthamine (GNT) was also separated to avoid interference with other ligands during docking and to ensure accurate identification of binding poses. Hydrogen atoms were added to approximate physiological pH conditions and to enable the formation of hydrogen bonds (Susanti *et al*., 2019).

Ligand preparation using YASARA showed that all ligands achieved optimal energy-minimized conformations and were stored in .pdb format. Energy minimization was performed to optimize ligand conformations and obtain the most stable structures prior to docking (Lukitaningsih *et al.,* 2013). A total of 163 test ligands were used, representing active compounds identified in red ginger. These ligands comprised vanilloid, terpenoid, flavonoid, and other compound classes (Zhang *et al*., 2022). In addition, Munadi (2018) reported that red ginger rhizomes originating from Indonesia contain bioactive compounds, including flavonoids, terpenoids, tannins, saponins, and alkaloids.

Grid box validation

Based on the validation results, the selected grid box size produced an RMSD value below 2 Å and was therefore considered valid. An RMSD value ≤ 2 Å indicates acceptable docking accuracy (Sari *et al.,* 2020). RMSD reflects the conformational deviation between the redocked native ligand and the ligand pose obtained from X-ray crystallography. The RMSD value obtained was close to zero, indicating a high degree of similarity and only minimal deviation between the redocked ligand and the crystallographic reference, thereby confirming the reliability of the docking protocol. Lower RMSD values indicate smaller deviations and higher similarity between the redocked and crystallographic ligand poses, whereas higher RMSD values indicate greater pose prediction errors (Sari *et al.,* 2020).

The selection of a 7 Å grid box was further supported by visualization results, which showed a strong overlap between the redocked ligand and the crystallographic ligand, confirming excellent structural agreement. Grid box parameters were determined based on the optimal combination of the lowest Gibbs free energy (ΔG) and the smallest RMSD value. Grid box validation is a critical preliminary step prior to virtual screening and molecular docking, as it defines the spatial region in which the ligand

explores conformational space within the target protein. During the redocking process, the target protein was treated as rigid to preserve the integrity of the active site, while the ligand was allowed to remain flexible, in accordance with standard docking protocols (Hasan *et al.,* 2022).

Virtual screening

The selection of ligands that passed the screening stage was based on ligands exhibiting ΔG values close to those of the native ligand and more negative than the reference ligand rivastigmine. An ideal drug candidate should demonstrate ΔG values comparable to the native and reference ligands in order to effectively compete for binding to the target receptor (Putri *et al.,* 2023). Baskaran *et al.* (2020) reported that rivastigmine exhibits relatively higher (less negative) ΔG values; therefore, ligands selected in this study were required to have more negative ΔG values than rivastigmine. A more negative ΔG relative to the reference ligand indicates stronger binding affinity toward the target receptor (Ferreira *et al.,* 2015). This selection threshold was applied to reduce the number of candidate ligands while ensuring the inclusion of characteristic bioactive compounds from red ginger.

Virtual screening was employed to identify the most promising drug candidates from a large compound library using computational approaches. Candidate selection was based on ligands exhibiting the most favorable interactions with the target protein and the lowest Gibbs free energy values generated during the screening process. Virtual screening is widely used in drug discovery because it is time-efficient, cost-effective, and flexible in execution (Muttaqin *et al.,* 2019). In addition to virtual screening, molecular docking represents another method for predicting optimal drug candidates. Virtual screening performs docking on multiple ligands simultaneously, whereas molecular docking evaluates one ligand per docking run. However, virtual screening generally offers lower specificity and accuracy than molecular docking. Therefore, ligands identified through virtual screening were subsequently subjected to molecular docking to enable more detailed and specific analysis of ligand–receptor interactions (Irsal *et al*., 2022).

The parameter evaluated in virtual screening was the Gibbs free energy (ΔG), which reflects the stability of the binding conformation between the receptor and ligand. ΔG values are generally negative (< 0), indicating the ability of a compound to bind to the target protein. More negative ΔG values correspond to increased reaction spontaneity. From a thermodynamic perspective, greater spontaneity indicates a more stable ligand–receptor complex and stronger binding interactions (Suhadi *et al.,* 2019). Ligands that passed the virtual screening stage were subsequently subjected to bioavailability and toxicity analyses for further selection as potential drug candidates.

Ligand bioavailability prediction

The 88 ligands that passed the virtual screening stage were subsequently subjected to bioavailability prediction. Three ligands—(2R,4S,5R)-2-(acetoxymethyl)-6-(2-methoxy-4-((E)-3-oxodec-4-en-1-yl)phenoxy)tetrahydro-2H-pyran-3,4,5-triyl triacetate, rutin, and (2R,4S,5R)-2-(acetoxymethyl)-6-(4-(5-hydroxy-3-oxodecyl)-2-methoxyphenoxy)tetrahydro-2H-pyran-3,4,5-triyl triacetate—violated more than two of Lipinski's Rule of Five and were therefore considered unsuitable as oral drug candidates. This limitation is primarily attributed to their low permeability, which hampers absorption and systemic distribution (Arwansyah & Hasrianti, 2014). These findings are consistent with an in silico study by Umara (2021), which reported that rutin exhibits low bioavailability due to

violations of four Lipinski criteria, rendering it unsuitable as an oral drug candidate.

The identification and development of potential drug candidates require evaluation of physicochemical properties and drug-like molecular characteristics, as these parameters determine solubility and permeability. An ideal drug must be efficiently absorbed, distributed, metabolized, and excreted by the body. One of the most widely used approaches for assessing drug-likeness is Lipinski's Rule of Five, which evaluates the likelihood of a compound exhibiting oral bioactivity in humans (Lipinski *et al.,* 2012).

Three ligands—(2R,4S,5R)-2-(acetoxymethyl)-6-(2-methoxy-4-((E)-3-oxodec-4-en-1-yl)phenoxy)tetrahydro-2H-pyran-3,4,5-triyl triacetate, rutin, and (2R,4S,5R)-2-(acetoxymethyl)-6-(4-(5-hydroxy-3-oxodecyl)-2-methoxyphenoxy)tetrahydro-2H-pyran-3,4,5-triyl triacetate—exhibited molecular weights greater than 500 Da. High molecular weight is associated with reduced membrane permeability, making it difficult for compounds to penetrate the lipid bilayer and be absorbed efficiently. As molecular weight increases, permeability generally decreases. A compound may be considered a viable drug candidate only if it can be metabolized after successfully traversing the lipid bilayer (Syahputra *et al.,* 2014).

Nine ligands—[8]-gingerdiol 3R,5S-diacetate, [10]-gingerdiol 3R,5S-diacetate, [6]-gingerdiol 3R,5S-diacetate, 3,5-diacetoxy-1-(4-hydroxy-3-methoxyphenyl)decane, (E)-1-(3-methoxy-4-(((3R,4S,6R)-3,4,5-trihydroxy-6-(hydroxymethyl)tetrahydro-2H-pyran-2-yl)oxy)phenyl)dec-4-en-3-one, rutin, histidine, (3R,5S)-[6]-gingerdiol, and 1-(4-hydroxy-3-methoxyphenyl)-3,5-decanediol—exhibited negative LogP values and were predicted to have difficulty penetrating the lipid bilayer.

According to Agustina & Kasmui (2021), negative LogP values indicated that compounds preferentially partition into polar phases, exhibit hydrophilic characteristics, and are easily distributed in polar environments but have limited ability to cross lipid membranes. Conversely, LogP values greater than five indicated high hydrophobicity and preferential distribution in nonpolar environments, which may result in prolonged retention within the lipid bilayer and hinder cellular uptake. Both extremes may prevent effective interaction with the target receptor. Therefore, ideal oral drug candidates should have LogP values below five but not negative, ensuring adequate solubility in both polar and nonpolar environments and facilitating efficient absorption and distribution (Rachmania *et al.,* 2015).

Two ligands—myricetin and rutin—exhibited hydrogen bond donor values greater than five. In addition, three ligands—(2R,4S,5R)-2-(acetoxymethyl)-6-(2-methoxy-4-((E)-3-oxodec-4-en-1-yl)phenoxy)tetrahydro-2H-pyran-3,4,5-triyl triacetate, rutin, and (2R,4S,5R)-2-(acetoxymethyl)-6-(4-(5-hydroxy-3-oxodecyl)-2-methoxyphenoxy)tetrahydro-2H-pyran-3,4,5-triyl triacetate—showed hydrogen bond acceptor values exceeding ten. According to Syahputra *et al*. (2014), these ligands are predicted to exhibit poor absorption, as higher hydrogen bonding capacity increases the energy required for membrane permeation. Excessive numbers of hydrogen bond donors and acceptors negatively affect compound permeability, particularly during transport across the lipid bilayer, thereby limiting cellular uptake (Lipinski *et al*., 2012). Compounds with fewer than five hydrogen bond donors and fewer than ten hydrogen bond acceptors generally require lower absorption energy compared with compounds that exceed these thresholds (Afandi *et al.,* 2022).

Furthermore, two ligands exhibited molar refractivity values greater than 140, while eighteen ligands showed molar refractivity values below 40. These ligands were predicted to have limited absorption potential. Molar refractivity reflects the total molar polarization of a compound and is influenced by pressure, refractive index, and temperature. This parameter represents the molecular distribution per mole of a compound and is commonly used to assess drug-likeness (Afandi *et al.,* 2022). According to Lipinski's Rule of Five, compounds with molar refractivity values within the range of 40–130 are considered optimal for efficient absorption in the human body (Lipinski *et al*., 2012).

Ligand toxicity prediction

The identification of compounds as potential drug candidates through in silico approaches requires toxicity assessment, even when the compounds originate from herbal plants that have been traditionally used for long periods. This is because such compounds are still considered foreign to the human body, and not all phytochemicals are inherently non-toxic. Toxicity analysis is therefore essential to ensure that a compound can be safely used as a therapeutic agent without inducing adverse effects. In this study, toxicity evaluation was conducted using four parameters: Human ether-a-go-go related gene (hERG) inhibition, carcinogenicity, chronic oral toxicity, and acute oral toxicity. Test ligands that violated any of these parameters were excluded as drug candidates due to their high toxicity and potential side effects (Djohari *et al*., 2022).

All tested ligands were classified as weak inhibitors in the hERG parameter, whereas the reference compound donepezil was identified as a strong inhibitor, indicating a higher risk of hERG channel blockade. This finding is consistent with the study by Marfira (2022), which reported that donepezil exhibits strong hERG inhibitory activity. Compounds classified as strong inhibitors are more likely to block the hERG channel, while weak inhibitors have a lower probability of interfering with hERG-mediated K^+ channel activity. An ideal drug candidate should not induce hERG blockade, as the hERG gene encodes a pore-forming subunit of the cardiac potassium channel that plays a critical role in maintaining normal heart rhythm (Lamothe *et al*., 2016). Inhibition of this channel may result in severe cardiac complications, including arrhythmia and sudden cardiac death. The probability value reflects the likelihood of a ligand exhibiting toxic behavior, where higher probability values indicate a lower toxic risk and better suitability as a drug candidate (Kalontong *et al.,* 2022).

The potential of donepezil to block hERG further highlights the importance of identifying alternative drug candidates with reduced side effects. Three ligands—α-farnesene, farnesal, and ethyl cinnamate—were identified as carcinogenic and were therefore excluded due to their potential cancer-inducing properties. These findings are consistent with in silico studies by Amelia (2019), which classified ethyl cinnamate as a carcinogenic compound, and by Safithri *et al.* (2022), which reported carcinogenic properties in farnesene derivatives. Carcinogenicity assessment is a toxicity test used to identify compounds capable of inducing cancer (Singgih *et al.,* 2019). According to the International Agency for Research on Cancer (IARC), carcinogenicity in humans is classified into four groups: Group 1 (carcinogenic), Group 2A (probably carcinogenic), Group 2B (possibly carcinogenic), Group 3 (not classifiable), and Group 4 (probably not carcinogenic) (Loomis *et al.,* 2018).

Chronic oral toxicity analysis demonstrated that all remaining ligands passed this criterion, indicating no predicted toxic effects following long-term exposure. This result aligns with the findings of Kendran *et al.*

(2013), which emphasize that suitable drug candidates should not produce harmful long-term side effects. Chronic oral toxicity evaluates adverse effects resulting from repeated administration over extended periods and is assessed using the lowest observed adverse effect level (LOAEL). The maximum recommended tolerated dose (MRTD), expressed in log(mg/kg/day), is used to predict tolerance levels. Compounds with MRTD values ≤ 0.477 log(mg/kg/day) are classified as chronic and associated with adverse effects, whereas MRTD values > 0.477 log(mg/kg/day) are considered non-chronic and unlikely to induce toxicity. Chronic toxicity effects are commonly associated with liver and kidney damage (Kendran *et al.,* 2013).

Seven ligands—myricetin, quercetin, fisetin, morin, kaempferol, naringenin, and the reference compound rivastigmine—were classified as acute oral toxicity category II. This finding is consistent with in silico studies by Syarafina *et al*. (2022), which reported that quercetin and kaempferol exhibit moderate toxicity and may induce gastrointestinal toxicity, cellular damage, and tissue injury, rendering them unsuitable as drug candidates at high doses. Similarly, Fakhruri *et al.* (2021) reported that naringenin belongs to the high-toxicity category II. Nevertheless, these ligands may still be considered potential drug candidates provided that their dosage is strictly limited to the range of 50–500 mg/kg. Increasing the dosage of toxic compounds may lead to severe physiological disturbances, including reduced motor activity and death (Musdalipah *et al.,* 2022). The toxic nature of rivastigmine further reinforces the need to identify safer alternative drug candidates.

Acute oral toxicity assessment was conducted to evaluate the toxic effects of compounds within 24 hours following oral administration (Kalontong *et al.,* 2022). The key parameter in this analysis is the median lethal dose (LD_{50}), which represents the estimated dose required to cause mortality in 50% of the test population. Lower LD_{50} values indicate higher toxicity, whereas higher LD_{50} values reflect lower toxic potential (Erhirhie et al., 2018). Acute oral toxicity is classified into four categories: Category I (LD_{50} < 500 mg/kg), which is considered toxic; Category III (500 mg/kg < LD_{50} < 5,000 mg/kg) and Category IV (LD_{50} > 5,000 mg/kg), which are considered non-toxic (Kalontong *et al*., 2022).

Ligand toxicity prediction

Ten ligands exhibited ΔG values that were highly consistent with the results obtained from virtual screening. The most favorable binding affinity was observed for myricetin, with a ΔG value of −10.9270 kcal/mol and an inhibition constant (Ki) of 0.0098 μM. In contrast, the weakest binding among the selected marker compounds was observed for [10]-gingerdiol 3R,5S-diacetate, which showed a ΔG value of −9.2700 kcal/mol and a Ki value of 0.1603 μM. Among all evaluated ligands, myricetin, quercetin, fisetin, and morin demonstrated the highest potential as drug candidates, as their ΔG values were closest to that of the natural ligand. These ligands exhibited competitive binding affinities relative to both the natural ligand and the reference compounds, indicating strong inhibitory potential against acetylcholinesterase. This finding is consistent with the study by Zheng & Polli (2010), which reported that compounds with Ki values below 100 μM are considered strong enzyme inhibitors.

Molecular docking was performed to predict the interactions between ligand molecules and the target protein, enabling the identification of optimal binding poses within the active site. This approach yields docking scores represented by Gibbs free energy (ΔG) and inhibition constant (Ki) values. Although molecular docking and virtual screening employ

similar computational principles, molecular docking involves the interaction of a single ligand per simulation and must therefore be performed iteratively. Re-docking is necessary to obtain more accurate docking scores and binding poses (Irsal *et al*., 2022). The inhibition constant (Ki) is directly correlated with ΔG; more negative ΔG values correspond to lower Ki values, and vice versa. Ki reflects the concentration of an inhibitor required to reduce the activity of the target enzyme. A lower Ki indicates higher inhibitory potency, whereas a higher Ki suggests reduced ligand effectiveness toward the receptor (Fakih *et al.,* 2022).

Key residue interactions

The test ligands [8]-gingerdiol 3R,5S-diacetate and [10]-gingerdiol 3R,5S-diacetate exhibited the highest number of interactions with amino acid residues, involving 21 and 23 residues, respectively. However, these interactions were dominated by hydrophobic and van der Waals contacts compared with other ligands. A greater number of hydrophobic and van der Waals interactions indicates enhanced ligand–receptor stability; nevertheless, these interactions are relatively weak and prone to dissociation (Arfi *et al.,* 2020). Myricetin and [8]-gingerdiol 3R,5S-diacetate also exhibited unfavorable donor–donor interactions, indicating the presence of undesirable and unstable ligand–receptor contacts (Ekawasti *et al.,* 2021).

Visualization analysis revealed several types of interactions, including hydrogen bonding, hydrophobic interactions, van der Waals forces, and unfavorable donor–donor interactions. Hydrophobic interactions comprised π–alkyl and alkyl contacts, whereas hydrogen bonding included conventional hydrogen bonds, π-donor hydrogen bonds, and carbon–hydrogen bonds (Ekawasti *et al.,* 2021). Hydrogen bonds arise from interactions between hydrogen atoms and highly electronegative atoms such as fluorine (F), oxygen (O), and nitrogen (N), and are considered strong and highly stable interactions (Ruslin et al., 2020). Hydrophobic interactions occur between nonpolar molecules in aqueous environments and are weaker than hydrogen bonds but stronger than van der Waals interactions. Van der Waals forces represent the weakest, nonspecific interactions arising from close atomic proximity (Ekawasti *et al.,* 2021).

Among the tested ligands, fisetin, morin, and kaempferol exhibited the highest number of hydrogen bonds with AChE residues and demonstrated strong binding interactions. This observation is consistent with the findings of Gholam *et al*. (2023), who reported that hydrogen bonds with distances shorter than 2.3 Å are considered strong and resistant to dissociation, thereby substantially enhancing binding affinity. An increased number of hydrogen bonds facilitates ligand binding and strengthens interactions with the receptor active site (Arfi *et al.,* 2020).

Acetylcholinesterase possesses two major binding regions: the catalytic active site (CAS) and the peripheral anionic site (PAS). The CAS is responsible for catalytic activity, whereas the PAS modulates enzyme function allosterically by altering the conformation of the binding pocket and the CAS (Genest *et al*., 2013). Fisetin, morin, and kaempferol exhibited strong binding to both CAS and PAS; however, fisetin and morin showed the most extensive interactions, particularly with HIS447 (CAS) and ASP74 and TYR72 (PAS). These dual-site interactions suggest superior inhibitory potential against AChE compared with other ligands. This observation is supported by Genest et al. (2013), who reported that compounds exhibiting dual binding site (DBS) interactions at both CAS and PAS possess high potential as promising drug candidates.

Fisetin and morin are also predicted to act as competitive inhibitors due to their binding

at the CAS. As reported by Syifa (2021), ligands that occupy the CAS function as competitive inhibitors by preventing substrate binding, whereas ligands interacting with the PAS act as noncompetitive inhibitors by binding to allosteric regions and inducing conformational changes in the enzyme. Binding at the CAS typically involves only one to two amino acid residues because the CAS is located deep within a narrow pocket approximately 20 Å in depth and 5 Å in width, limiting ligand accessibility (Cheng *et al.,* 2017). Nevertheless, PAS binding at the pocket entrance contributes significantly to effective AChE inhibition (Genest *et al.,* 2013).

Overall, the amino acid interaction profiles indicate that fisetin and morin are highly promising acetylcholinesterase inhibitors for dementia therapy. In addition to extensive residue interactions, both ligands exhibited ΔG values closest to that of the natural ligand and more negative than those of the reference compounds. These findings are supported by in vivo evidence from Khatoon *et al.* (2023), who demonstrated increased neurotransmitter levels following fisetin administration in mice via AChE inhibition. Furthermore, in silico analysis by Remya *et al.* (2012) confirmed that morin effectively reduces AChE activity through direct binding to the enzyme's active site.

Two tested ligands, fisetin and morin, were identified as highly promising candidates for dementia therapy. Both ligands exhibited Gibbs free energy (ΔG) and inhibition constant (Ki) values comparable to the natural ligand galanthamine and more favorable (more negative) than those of the reference inhibitors donepezil and rivastigmine. These ligands demonstrated strong interactions with key residues at the catalytic active site (CAS), particularly HIS447, and with the peripheral anionic site (PAS) residues ASP74 and TYR72. Binding at the CAS suggests that fisetin and morin may function as competitive inhibitors, thereby effectively suppressing acetylcholinesterase (AChE) activity for dementia treatment. In addition, both ligands exhibited favorable solubility and were predicted to be non-toxic, supporting their suitability as drug candidates.

Active compounds identified as potential AChE inhibitors through in silico analysis require further investigation, including molecular dynamics simulations and experimental validation through in vitro and in vivo studies. These follow-up studies are necessary to confirm inhibitory potency, binding stability, and the specific inhibition mechanisms of the test ligands against acetylcholinesterase.

REFERENCES

Abusham, R. A. K., Masomian, M., Salleh, A. B., Leow, A. T. C., & Rahman, R. N. Z. R. A. (2019). An *in silico* approach to understanding the structure–function relationship: A molecular dynamics simulation study of Rand serine protease properties from *Bacillus subtilis* in aqueous solvents. *Advances in Biotechnology & Microbiology*, *12*(2), 1–10. https://doi.org/10.19080/AIBM.2019.12.555834

Afandi, Z., Rahmayanti, Y., & Rizarullah, R. (2022). Identification of potential antivirals from *Moringa oleifera* leaf as SARS-CoV-2 Mpro inhibitors: A molecular docking study. *Chimica Didactica Acta*, *10*(1), 1–9. https://doi.org/10.24815/jcd.v10i1.24565

Agistia, D. D., Purnomo, H., Tegar, M., & Nugroho, A. E. (2013). Interaction between active compounds from *Aegle marmelos* Correa as anti-inflammatory agents with COX-1 and COX-2 receptors. *Traditional Medicine Journal*, *18*(2), 80–87.

Agustina, L., & Kasmui, K. (2021). Computational study of xanthone derivative compounds as anticancer agents against chronic myeloid leukemia K562. *Indonesian Journal of Mathematics and Natural Sciences*, *44*(1), 1–11. https://doi.org/10.15294/ijmns.v44i1.32702

Amelia, R. (2019). *Analisis penambatan molekul senyawa aktif kayu manis (Cinnamon) pada*

enzim MGA untuk agen antidiabetes [Undergraduate thesis, Institut Pertanian Bogor].

Arfi, A. S., Lestari, R. D., & Damayanti, D. S. (2020). *In silico* study of active compounds from turmeric rhizome (*Curcuma domestica*) on acetylcholinesterase inhibition, β-tubulin microtubules, and calcium channel activation as anthelmintic therapy. *Jurnal Kedokteran Komunitas*, *8*(2), 36–47.

Aryanta, I. W. R. (2019). Health benefits of ginger. *Widya Kesehatan*, *1*(2), 39–43. https://doi.org/10.32795/widyakesehatan.v1i2.463

Arwansyah, & Hasrianti. (2014). Molecular docking simulation of curcumin and its analogs as selective androgen receptor modulators (SARMs) in prostate cancer. *Jurnal Dinamika*, *5*(2), 60–75.

Atanasova, M., Yordanov, N., Dimitrov, I., Berkov, S., & Doytchinova, I. (2015). Molecular docking study on galantamine derivatives as cholinesterase inhibitors. *Molecular Informatics*, *34*(6–7), 394–403. https://doi.org/10.1002/minf.201400145

Baskaran, K. P., Arumugam, A., Kandasamy, R., & Alagarsamy, S. (2020). *In silico* prediction of maximum binding affinity and ligand–protein interaction studies on Alzheimer's disease. *International Journal of Research – GRANTHAALAYAH*, *8*(11), 362–370. https://doi.org/10.29121/granthaalayah.v8.i11.2020.2472

Chen, Y. X., Li, G. Z., Zhang, B., Xia, Z. Y., & Zhang, M. (2016). Molecular evaluation of herbal compounds as potent inhibitors of acetylcholinesterase for the treatment of Alzheimer's disease. *Molecular Medicine Reports*. https://doi.org/10.3892/mmr.2016.5244

Cheng, S., Song, W., Yuan, X., & Xu, Y. (2017). Gorge motions of acetylcholinesterase revealed by microsecond molecular dynamics simulations. *Scientific Reports*, *7*(1), 1–12. https://doi.org/10.1038/s41598-017-03088-y

Cheung, J., Rudolph, M. J., Burshteyn, F., Cassidy, M. S., Gary, E. N., Love, J., Franklin, M. C., & Height, J. J. (2012). Structures of human acetylcholinesterase in complex with pharmacologically important ligands. *Journal of Medicinal Chemistry*, *55*(22), 10282–10286. https://doi.org/10.1021/jm300871x

Colović, M. B., Krstić, D. Z., Lazarević-Pašti, T. D., Bondžić, A. M., & Vasić, V. M. (2013). Acetylcholinesterase inhibitors: Pharmacology and toxicology. *Current Neuropharmacology*, *11*(3), 315–335. https://doi.org/10.2174/1570159X11311030006

Daina, A., Michielin, O., & Zoete, V. (2017). SwissADME: A free web tool to evaluate pharmacokinetics, drug-likeness, and medicinal chemistry friendliness of small molecules. *Scientific Reports*, *7*, 1–13. https://doi.org/10.1038/srep42717

Del-Aguila, J. L., Koboldt, D. C., Black, K., Chasse, R., Norton, J., Wilson, R. K., & Cruchaga, C. (2015). Alzheimer's disease: Rare variants with large effect sizes. *Current Opinion in Genetics & Development*, *33*, 49–55. https://doi.org/10.1016/j.gde.2015.07.008

Djohari, M., Efendi, T. T., Rahmawati, N., Husnawati, & Aryani, F. (2022). Acute and delayed toxicity tests of the butanol fraction of kaik-kaik root leaves (*Uncaria cordata* (Lour.) Merr.) in white mice (*Mus musculus* L.). *Jurnal Ilmiah Ibnu Sina: Ilmu Farmasi dan Kesehatan*, *7*(1), 203–211. https://doi.org/10.36387/jiis.v7i1.874

Dvir, H., Silman, I., Harel, M., Rosenberry, T. L., & Sussman, J. L. (2010). Acetylcholinesterase: From 3D structure to function. *Chemico-Biological Interactions*, *187*(1–3), 10–22. https://doi.org/10.1016/j.cbi.2010.01.042

Dwivedi, C., Chandrakar, K., Singh, V., Tiwari, S. P., Satapathy, T., Kesharwani, S., Kumar, B., & Roy, A. (2014). Indian herbal medicines used for the treatment of dementia: An overview. *International Journal of Pharmacognosy*, *1*(9), 553–571. https://doi.org/10.13040/IJPSR.0975-8232.IJP.1(9).553-71

Ekawasti, F., Sa'diah, S., Cahyaningsih, U., Dharmayanti, N. L. P. I., & Subekti, D. T. (2021). Molecular docking of red ginger and turmeric compounds on dense granule protein-1 of *Toxoplasma gondii* using *in silico* methods. *Jurnal Veteriner*, *22*(4), 474–484.

https://doi.org/10.19087/jveteriner.2021.22.4.474

Fakhruri, M., Rahmayanti, Y., & Isfanda. (2021). Phytochemical potential of *Citrus aurantium* (hesperetin, naringenin) in inhibiting xanthine oxidase in hyperuricemia: An *in silico* study. *Journal of Health Sciences*, *2*(1), 79–89.

Fakih, T. M., Putri, N. W. R. P., Marillia, V., Ramadhan, D. S. F., & Darusman, F. (2022). Identification of biological activity, toxicity prediction, and molecular docking of jubanine compound from *Ziziphus spina-christi* as a SARS-CoV-2 antiviral candidate. *Jurnal Riset Kimia*, *13*(1), 111–121. https://doi.org/10.25077/jrk.v13i1.437

Ferreira, L. G., Dos Santos, R. N., Oliva, G., & Andricopulo, A. D. (2015). Molecular docking and structure-based drug design strategies. *Molecules*, *20*(7), 13384–13421. https://doi.org/10.3390/molecules200713384

Ferreira-Vieira, T. H., Guimarães, I. M., Silva, F. R., & Ribeiro, F. M. (2016). Alzheimer's disease: Targeting the cholinergic system. *Current Neuropharmacology*, *14*(1), 101–115. https://doi.org/10.2174/1570159X13666150716165726

Fitri, M., Rahmi, U., Pitriani, P., & Sulastri, A. (2020). Effectiveness of brain vitalization exercise on physical fitness in elderly patients with dementia. *Jurnal Sport: Jurnal Penelitian Pembelajaran*, *6*(2), 364–374. https://doi.org/10.29407/js_unpgri.v6i2.14360

Genest, D., Rochais, C., Lecoutey, C., De Oliveira Santos, J. S., Ballandonne, C., Butt-Gueulle, S., Legay, R., Sinče, M., & Dallemagne, P. (2013). Design, synthesis and biological evaluation of novel indano- and thiaindano-pyrazoles with potential interest for Alzheimer's disease. *MedChemComm*, *4*(6), 925–931. https://doi.org/10.1039/C3MD00041A

Ghasemzadeh, A., Jaafar, H. Z. E., & Rahmat, A. (2010). Antioxidant activities, total phenolics and flavonoids content in two varieties of Malaysian young ginger (*Zingiber officinale* Roscoe). *Molecules*, *15*(6), 4324–4333. https://doi.org/10.3390/molecules15064324

Gholam, G. M., Darmawan, N. I., Siregar, J. E., & Artika, I. M. (2023). Selected polyphenols from date (*Phoenix dactylifera*) as anti-virulence agents of *Candida albicans* through multiple enzyme targets. *Biointerface Research in Applied Chemistry*, *13*(4), 1–19. https://doi.org/10.33263/BRIAC134.386

Greenidge, P. A., Kramer, C., Mozziconacci, J. C., & Wolf, R. M. (2013). MM/GBSA binding energy prediction on the PDBbind data set: Successes, failures, and directions for further improvement. *Journal of Chemical Information and Modeling*, *53*(1), 201–209. https://doi.org/10.1021/ci300425v

Gultom, R., Martina, S. E., & Harianji, E. S. (2021). Implementation of reminiscence therapy as an effort to prevent dementia in the elderly at the Social Services Unit for Older Adults, Binjai. *Jurnal Pengabdian Masyarakat*, *4*(2), 122–128. https://doi.org/10.32529/tano.v4i2.1006

Hasan, R., I'anah, F. C., & Bahi, R. R. R. (2022). Molecular docking of potential compounds from *Moringa oleifera* leaves against folate receptors. *Journal of Innovation Research and Knowledge*, *2*(2), 519–526.

Hatmanti, N. M., & Yunita, A. (2019). Elderly exercise and puzzle therapy on dementia in older adults. *Jurnal Keperawatan Muhammadiyah*, *4*(1), 104–107. https://doi.org/10.30651/jkm.v4i1.2422

Irsal, R. A. P., Seno, D. S. H., Safitri, M., & Kurniasih, R. (2022). Molecular docking of active compounds from red betel (*Piper crocatum*) as angiotensin-converting enzyme inhibitors. *Jurnal Farmamedika*, *7*(2), 104–113.

Kalontong, P. K., Safithri, M., & Tarman, K. (2022). Molecular docking of active compounds from *Spirulina platensis* as TMPRSS2 inhibitors to prevent SARS-CoV-2 infection. *Jurnal Pengolahan Hasil Perikanan Indonesia*, *25*(2), 253–267. https://doi.org/10.17844/jphpi.v25i2.40645

Kanwar, G., Kumar, A., & Mahajan, A. (2018). Open-source software tools for computer-aided drug design. *International Journal of Research in Pharmaceutical Sciences*, *9*(1), 86–95.

Kendran, A. A. S., Gelgel, K. T. P., Pertiwi, N. W. L., Anthara, M. S., Dharmayuda, A. A. G. O., & Anggreni, L. D. (2013). Toxicity of

red betel leaf extract in white rats with diabetes mellitus. *Jurnal Veteriner*, *14*(4), 527–533.

Khatoon, S., Samim, M., Dahalia, M., & Nidhi. (2023). Fisetin provides neuroprotection in pentylenetetrazole-induced cognitive impairment by upregulating CREB/BDNF. *European Journal of Pharmacology*, *944*(1), 175583. https://doi.org/10.1016/j.ejphar.2023.175583

Laksmiani, N. P. L., Larasanty, L. P. F., Santika, A. A. G. J., Prayoga, P. A. A., Dewi, A. A. I. K., & Dewi, N. P. A. K. (2020). Activity of active compounds from medicinal plants against SARS-CoV-2 using *in silico* assay. *Biomedical & Pharmacology Journal*, *13*(2), 873–881. https://doi.org/10.13005/BPJ/1953

Lamothe, S. M., Guo, J., Li, W., Yang, T., & Zhang, S. (2016). The human ether-à-go-go–related gene (hERG) potassium channel represents an unusual target for protease-mediated damage. *Journal of Biological Chemistry*, *291*(39), 20387–20401. https://doi.org/10.1074/jbc.M116.743138

Land, H., & Humble, M. S. (2018). YASARA: A tool to obtain structural guidance in biocatalytic investigations. *Protein Engineering*, *1*(3), 43–67. https://doi.org/10.1007/978-1-4939-7366-8_4

Lipinski, C. A., Lombardo, F., Dominy, B. W., & Feeney, P. J. (2012). Experimental and computational approaches to estimate solubility and permeability in drug discovery and development settings. *Advanced Drug Delivery Reviews*, *64*(1), 4–17. https://doi.org/10.1016/j.addr.2012.09.019

Loizzo, M. R., Bonesi, M., Pugliese, A., Menichini, F., & Tundis, R. (2014). Chemical composition and bioactivity of dried fruits and honey of *Ficus carica* cultivars Dottato, San Francesco and Citrullara. *Journal of the Science of Food and Agriculture*, *94*(11), 2179–2186. https://doi.org/10.1002/jsfa.6533

Loomis, D., Guha, N., Hall, A. L., & Straif, K. (2018). Identifying occupational carcinogens: An update from the IARC monographs. *Occupational and Environmental Medicine*, *75*(8), 593–603. https://doi.org/10.1136/oemed-2017-104944

Lukitaningsih, E., Mustikawaty, A. A., & Sudarmanto, A. (2013). Homology modeling and molecular docking of active compounds from yam bean (*Pachyrrhizus erosus*) as tyrosinase inhibitors in *Homo sapiens*. *Jurnal Ilmu Kefarmasian Indonesia*, *11*(2), 134–141.

Madan, R., Pandit, K., Kumar, H., Kumari, N., & Singh, S. (2021). Principles and aspects of molecular docking: A bird's-eye view. *Hans Shodh Sudha*, *1*(1), 110–121.

Marfira, N. (2022). *Potensi ekstrak metanol, etanol, dan minyak jintan hitam (Nigella sativa) sebagai inhibitor asetilkolinesterase* [Undergraduate thesis, Institut Pertanian Bogor].

Munadi, R. (2018). Chemical component analysis and antioxidant activity of red ginger (*Zingiber officinale* Rosc. var. *rubrum*) rhizome extract. *Cokroaminoto Journal of Chemical Science*, *2*(1), 1–6.

Musdalipah, Yodha, A. W. M., Karmilah, Tee, S. A., Reymon, Daud, N. S., Setiawan, M. A., Badia, E., & Agustini. (2022). Acute toxicity and lethal dose (LD_{50}) of walay fruit (*Meistera chinensis*) extract from Southeast Sulawesi in mice (*Mus musculus*). *Pharmacoscript*, *5*(2), 186–197.

Muttaqin, F. Z., Astuti, W. A. P., Aman, L. O., Febrina, E., & Asnawi, A. (2019). Structure-based virtual screening of the ZINC natural product database as Bruton tyrosine kinase inhibitors. *Jurnal Ilmiah Ibnu Sina*, *4*(2), 400–409.

Nishidono, Y., Saifudin, A., Deevanhxay, P., & Tanaka, K. (2020). Metabolite profiling of ginger (*Zingiber officinale* Roscoe) using GC–MS and multivariate statistical analysis. *Journal of the Asia-Japan Research Institute, Ritsumeikan University*, *2*(1), 1–14.

Noorsy, W. A. (2022). *Potensi flavonoid hasil similarity search isoliquiritigenin dalam inhibisi FMS-like tyrosine kinase-3 (FLT3) secara in silico* [Undergraduate thesis, Institut Pertanian Bogor].

Oboh, G., Ademiluyi, A. O., & Akinyemi, A. J. (2012). Inhibition of acetylcholinesterase activities and some pro-oxidant–induced lipid peroxidation in rat brain by two varieties of ginger (*Zingiber officinale*).

Experimental and Toxicologic Pathology, *64*(4), 315–319. https://doi.org/10.1016/j.etp.2010.09.004

Ochieng, P. J., Sumaryada, T., & Okun, D. (2017). Molecular docking and pharmacokinetic prediction of herbal derivatives as maltase–glucoamylase inhibitors. *Asian Journal of Pharmaceutical and Clinical Research*, *10*(9), 392–398. https://doi.org/10.22159/ajpcr.2017.v10i9.19337

Pratama, R. (2015). *Penambatan molekuler senyawa aktif temulawak (Curcuma xanthorrhiza) dengan enzim COX-2 sebagai kandidat obat antikanker payudara* [Undergraduate thesis, Institut Pertanian Bogor].

Putri, R. G., Safithri, M., Husnawati, & Kurniasih, R. (2023). Molecular docking of active compounds from red betel (*Piper crocatum*) on butyrylcholinesterase as anti-Alzheimer's candidates. *Alchemy: Journal of Chemistry Research*, *19*(1), 68–85. https://doi.org/10.20961/alchemy.19.1.59676.68-85

Rachmania, R. A. (2019). Validation of screening protocols and interaction analysis of natural product-based antiproliferative inhibitors against cyclin-dependent kinase 4 (CDK4). *Media Farmasi: Jurnal Ilmu Farmasi*, *16*(1), 21. https://doi.org/10.12928/mf.v16i1.12101

Rachmania, R. A., Supandi, & Larasati, O. A. (2015). *In silico* analysis of diterpenoid lactone compounds from sambiloto herb (*Andrographis paniculata* Nees) on α-glucosidase receptor as type II antidiabetic agents. *Pharmacy*.

Remya, C., Dileep, K. V., Tintu, I., Variyar, E. J., & Sadasivan, C. (2012). Design of potent inhibitors of acetylcholinesterase using morin as the starting compound. *Frontiers in Life Science*, *6*(3–4), 107–117. https://doi.org/10.1080/21553769.2013.815137

Rinanda, T., Isnanda, R. P., & Zulfitri. (2018). Chemical analysis of red ginger (*Zingiber officinale* Roscoe var. *rubrum*) essential oil and its anti-biofilm activity against *Candida albicans*. *Natural Product Communications*, *13*(12), 1587–1590. https://doi.org/10.1177/1934578X1801301206

Ruslin, Yana, N. R. A., & Leorita, M. (2020). Design of leonurine derivatives as anti-inflammatory drug candidates. *Jurnal Farmasi Galenika*, *6*(1), 181–191. https://doi.org/10.22487/j24428744.2020.v6.i1.15025

Safithri, M., Miantika, S., & Ambarsari, L. (2022). *In silico* analysis of active compounds from red betel (*Piper crocatum*) as xanthine oxidase inhibitors. *Current Biochemistry*, *9*(2), 51–62.

Safwan, S., Yuliani, S., & Pramono, S. (2014). Activity test of turmeric (*Curcuma longa* Linn.) rhizome essential oil in Sprague Dawley rats with dementia model (acetylcholinesterase inhibition study). *Kartika: Jurnal Ilmiah Farmasi*, *2*(2), 20–26. https://doi.org/10.26874/kjif.v2i2.29

Sağlık, B. N., Levent, S., Osmaniye, D., Çevik, U. A., Çavuşoğlu, B. K., Özkay, Y., Koparal, A. S., & Kaplancıklı, Z. A. (2020). Design, synthesis, and biological activity evaluation of new donepezil-like compounds bearing thiazole ring for the treatment of Alzheimer's disease. *Crystals*, *10*(8), 1–17. https://doi.org/10.3390/cryst10080637

Sari, I. W., Junaidin, J., & Pratiwi, D. (2020). Molecular docking study of flavonoid compounds from cat's whiskers herb (*Orthosiphon stamineus* B.) on α-glucosidase receptor as type 2 antidiabetic agents. *Jurnal Farmagazine*, *7*(2), 54–60. https://doi.org/10.47653/farm.v7i2.194

Singgih, M., Permana, B., Maulidya, S. A. I., & Yuliana, A. (2019). *In silico* study of secondary metabolites from *Monascus* sp. as anticholesterol and anticancer drug candidates. *Alchemy: Journal of Chemistry Research*, *15*(1), 104–123. https://doi.org/10.20961/alchemy.15.1.25294

Smart, O. S., Horský, V., Gore, S., Svobodová Vařeková, R., Bendová, V., Kleywegt, G. J., & Velankar, S. (2018). Worldwide Protein Data Bank validation information: Usage and trends. *Acta Crystallographica Section D: Structural Biology, 74*(3), 237–244. https://doi.org/10.1107/S2059798318001307

Suciyati, S. W., & Adnyana, I. K. (2017). Red ginger (*Zingiber officinale* Roscoe var. *Rubrum*): A review. *Pharmacologyonline, 2*(1), 60–65.

Suhadi, A., Rizarullah, R., & Feriyani, F. (2019). Simulasi docking senyawa aktif daun binahong sebagai inhibitor enzim aldose reductase. *Jurnal Penelitian Kesehatan, 6*(2), 55–65. https://doi.org/10.22435/sel.v6i2.1651

Susanti, N. M. P., Laksmiani, N. P. L., Noviyanti, N. K. M., Arianti, K. M., & Duantara, I. K. (2019). Molecular docking terpinen-4-ol sebagai antiinflamasi pada aterosklerosis secara *in silico*. *Jurnal Kimia, 13*(2), 221–228. https://doi.org/10.24843/jchem.2019.v13.i02.p16

Syahputra, G., Ambarsari, L., & T., S. (2014). Simulasi docking kurkumin enol, bisdemetoksikurkumin dan analognya sebagai inhibitor enzim 12-lipoksigenase. *Biofisika, 10*(1), 55–67.

Syarafina, Z. Y. I., Safithri, M., Bintang, M., & Kurniasih, R. (2022). *In silico* screening of cinnamon (*Cinnamomum burmannii*) bioactive compounds as acetylcholinesterase inhibitors. *Jurnal Kimia Sains dan Aplikasi, 25*(3), 97–107. https://doi.org/10.14710/jksa.25.3.97-107

Syifa, K. (2021). *Analisis potensi senyawa aktif daun sirih merah (Piper crocatum) sebagai inhibitor enzim asetilkolin esterase secara in silico* [Undergraduate thesis]. Institut Pertanian Bogor.

Tuzimski, T., & Petruczynik, A. (2022). Determination of anti-Alzheimer's disease activity of selected plant ingredients. *Molecules, 27*(10), Article 3222. https://doi.org/10.3390/molecules27103222

Umara, A. (2021). *Pengikatan senyawa flavonoid daun jati belanda dan salam dengan protein B-cell lymphoma-2 menginduksi apoptosis sel makrofag secara in silico* [Undergraduate thesis]. Institut Pertanian Bogor.

Wattanathorn, J., Jittiwat, J., Tongun, T., Muchimapura, S., & Ingkaninan, K. (2011). *Zingiber officinale* mitigates brain damage and improves memory impairment in focal cerebral ischemic rat. *Evidence-Based Complementary and Alternative Medicine*, Article 429505. https://doi.org/10.1155/2011/429505

World Health Organization. (2017, December 7). *Dementia: Number of people affected to triple in next 30 years*. https://www.who.int/news/item/07-12-2017-dementia-number-of-people-affected-to-triple-in-next-30-years

World Health Organization. (2020). *The top 10 causes of death*. https://www.who.int/news-room/fact-sheets/detail/the-top-10-causes-of-death.

Zhang, S., Kou, X., Zhao, H., Mak, K. K., Balijepalli, M. K., & Pichika, M. R. (2022). *Zingiber officinale* var. *Rubrum*: Red ginger's medicinal uses. *Molecules, 27*(3), Article 775. https://doi.org/10.3390/molecules27030775

Zheng, X., & Polli, J. E. (2010). Identification of inhibitor concentrations to efficiently screen and measure inhibition *K*i values against solute carrier transporters. *European Journal of Pharmaceutical Sciences, 41*(1), 43–52. https://doi.org/10.1016/j.ejps.2010.05.013

Zhou, Y., Wang, S., & Zhang, Y. (2010). Catalytic reaction mechanism of acetylcholinesterase determined by Born–Oppenheimer *ab initio* QM/MM molecular dynamics simulations. *The Journal of Physical Chemistry B, 114*(26), 8817–8825. https://doi.org/10.1021/jp104258d

Zuraida, A. R., Shukri, M. M. A., Sabrina, E. M. N., Nazreena, A. O., Radziah, C. C. Z., Pavallekoodi, G., & Sreeramanan, S. (2016). Micropropagation of ginger (*Zingiber officinale* var. *Rubrum*) using buds from microshoots. *Pakistan Journal of Botany, 48*(3), 1153–1158.